Chemistry and Materials

The Center for Science Innovation

Research Article *Chem. Mater. 4(2) 2025, 72-78*

Tunable Film Density of Electrodeposited Gold Nanoparticles for Enhanced Antioxidant Activity

B. Asih Suliasih[1]*, Charzen Mae Kinoan[2]

[1]Centre for Drug Delivery Technology and Vaccine, Faculty of Pharmacy, Universiti Kebangsaan Malaysia, Kuala Lumpur 50300, Malaysia

[2]College of pharmacy and Medical Technology, University of San Agustin, Iloilo City, 5000 Iloilo, Philippines

*Corresponding author: p113963@siswa.ukm.edu.my

Received
30 May 2025

Received in revised form
13 June 2025

Accepted
25 June 2025

Published online
30 June 2025

DOI
https://doi.org/10.56425/4q3vyc49

Abstract

The synthesis of gold nanoparticles (AuNPs) is a critical aspect in the development of large-scale antioxidant nanomaterials. Although, biological methods offer a non-toxic reagent and an environmentally friendly route for synthesis. However, their scalability is limited by the non-uniformity of particle size, the scarcity of biological materials, the challenges associated with controlling organism growth, and the relatively long synthesis time. Therefore, chemical methods, especially electrodepositions, are preferred due to their effectiveness, efficiency, and the ability to precisely control particle size and shape through electrolyte modifications. In this study, two supporting electrolytes, KCl and Na_2SO_4, were employed. The results demonstrated that the type of electrolyte ion significantly influences the particle density of the AuNPs, with KCl electrolyte providing a higher particle density. This increased particle density correlates with a larger active surface area per unit area, subsequently enhancing the antioxidant activity of the AuNPs, as evidenced by up to 57% DPPH inhibition. Furthermore, cytotoxicity and cytoprotective assays indicated good biocompatibility and protective capabilities of AuNPs.

Keywords: AuNPs, supporting electrolyte, particle density, antioxidant activity

1. Introduction

Degenerative diseases are caused by elevated concentrations of free radicals from both external and internal sources [1,2]. The external factors that cause free radicals to arise include air pollution, water contamination, unhealthy food and beverages, pesticides, cigarette smoke, solar radiation, and electromagnetic waves [3]. Meanwhile, the internal factors come from the respiratory processes of cellular metabolism by mitochondria [4].

Free radicals are a group of atoms or molecules that are highly reactive and unstable due to the presence of one or more unpaired electrons in their outer orbital [5]. These unpaired electrons trigger oxidative reactions within the body, leading to damage to biological components [6]. Damage caused by free radicals can be mitigated through the use of antioxidant compounds [7]. Antioxidants help to prevent biological damage due to their ability to neutralize free radicals [8].

Antioxidant compounds can be derived from both natural and synthetic sources. Natural antioxidants can be obtained from vegetables, fruits, and spices rich in vitamins, phenolic compounds, carotenoids, and other micronutrients [9]. Natural antioxidants possess advantages such as abundant availability in nature, minimal side effects, and ease of absorption by the body [10]. However, natural antioxidants also have several limitations, including instability, limited concentrations, and challenges in large-scale production [11]. Consequently, synthetic antioxidant materials such as butylated hydroxyanisole (BHA) and butylated hydroxytoluene (BHT) have been studied [12]. Nevertheless, BHA exhibits cytotoxic properties that can damage normal cells, while BHT is carcinogenic due to its potential to cause DNA destruction [13]. Therefore, there

is a need for alternative synthetic antioxidants to address these issues.

Nanotechnology presents opportunities for the development and enhancement of antioxidant material effectiveness [14]. Nanoscale diameters provide significant benefits for antioxidant activity, such as high active surface area, good stability, and the ability to specifically target free radicals [9]. Among various nanomaterials, gold nanoparticles (AuNPs) have attracted considerable attention due to their extremely small size, high surface area, stability, non-toxicity, and favorable physical and chemical properties [15]. Controlling the shape, size, and density of AuNPs is crucial for enhancing the antioxidant activity of these materials [16]. Hence, the selection of appropriate synthesis methods is a key consideration in synthesizing these materials.

Several synthesis methods of AuNPs have been conducted, including biological and chemical methods [17,18]. Biological approaches use non-toxic solvent chemicals and are environmentally friendly. However, the biological technique has disadvantages due to the scarcity of biological materials, the long synthesis time, the difficulty in controlling the growth of living organisms, and the non-uniformity of particle size [16]. On the other hand, chemical methods, especially electrodeposition methods, an effective and efficient synthesis method, offer good control over the shape, size, and density by simply adjusting synthesis parameters such as current, voltage, time, and the adjustment of electrolyte modifications [19–21].

Electrolyte modification in the synthesis of AuNPs can be achieved by adding a supporting electrolyte. Zakaria et al. [22] investigated how different electrolytes, each containing KNO_3, HNO_3, H_2SO_4, and $NaNO_3$, influence morphological alteration and the distribution of AuNPs. It was found that the main factors affecting the electrochemical performance of various electrolyte solutions are ionic properties and stability, which can influence interactions between electrodes.

Supporting electrolyte agents such as KCl and Na_2SO_4 might be beneficial for electrodeposition AuNPs. Both KCl and Na_2SO_4 are neutral salts that are non-toxic. The ions of salts can enhance the conductivity of the electrolyte, provide electrostatic stabilization that prevents nanoparticle agglomeration, resulting in uniformly sized nanoparticles [23–25]. Therefore, in this study, the synthesis of AuNPs was conducted in two different electrolytes. The results showed that supporting electrolytes significantly influenced particle density. Higher particle density yields a larger active surface area within the same coverage area, which impacts the antioxidant activity of the AuNPs.

2. Materials and Methods

2.1 Materials

Chemicals employed were tetrachloroauric(III) acid trihydrate ($HAuCl_4.3H_2O$, 99.9%, Sigma Aldrich), aquabidestilled, potassium chloride (KCl, 99.0%, Merck), sodium sulfate (Na_2SO_4, 99.0%, Merk), ethanol pro analysis (C_2H_5OH, 96%, Merck), DPPH ($C_{18}H_{12}N_5O_6$, 90.0%, Sigma Aldrich), vitamin C, fluorouracil (FU).

2.2 Methods

2.2.1 Synthesis of AuNPs with electrodeposition

Distinct electrolyte solutions were prepared, the first containing 1 mM $HAuCl_4{\cdot}3H_2O$ in 100 mM KCl (AuNPs 1), and the second comprising the same gold precursor concentration but in 100 mM Na_2SO_4 (AuNPs 2). The substrate was cleaned with ethanol and aquabidestilation. Cyclic voltammetry was employed as the electrodeposition technique using a three-electrode configuration, with Ag/AgCl as the reference electrode, Pt as the counter electrode, and an ITO-PET substrate as the working electrode. Deposition was conducted for 160 cycles within a potential range of -1 V to -1.5 V at a scan rate of 125 mV/s. The resulting films were dried at ambient temperature.

2.2.2 Characterization

The phase composition and crystallinity of the material were characterized using an X-ray diffractometer (XRD, Rigaku). Subsequently, the morphology, size, and distribution of the particles were characterized employing scanning electron microscopy (SEM, JEOL JSM-6510).

2.2.3 Antioxidant activity test

The antioxidant activity of the AuNPs was assessed using the DPPH assay. AuNPs film samples were incubated in a microplate containing DPPH solution with a concentration of 39 µg/mL ethanol-based solution. Absorbance measurements were conducted utilizing a microplate reader coupled with UV-Vis spectroscopy at a wavelength of 300-720 nm. The antioxidant activity was quantified by calculating the percentage inhibition according to the following equation 1.

$$\%inhibition = \frac{\text{Abs control} - \text{Abs sample}}{\text{Abs control}} \times 100\% \quad (1)$$

The Abs control represents the maximum absorbance value of DPPH, while the Abs sample denotes the

maximum absorbance value of the AuNPs sample after the addition of DPPH.

2.2.4 Cytotoxicity and cytoprotective assay

2.2.4.1 Cell culture

HaCaT cells were cultured in Dulbecco's Modified Eagle Medium (DMEM) supplemented with 10% fetal bovine serum (Gibco, USA) and 1% penicillin-streptomycin solution. The cells were maintained in a humidified incubator at 37°C with 5% CO_2 (ThermoScientific, USA). Cultures were passaged once they reached 90%–100% confluency. Cells were harvested using a 0.25% trypsin-EDTA solution (Gibco, USA).

2.2.4.2 Sample preparation

Sample solutions were prepared by immersing gold-platinum nanofilms (AuPtNFs) in 48-well culture plates containing 400 µL of DMEM. The immersion was conducted for 72 hours in a humidified incubator maintained at 37°C with 5% CO_2.

2.2.4.3 Cytotoxicity assay

HaCaT cells were seeded at a density of 1×10^4 cells per well in a 96-well plate and incubated for 24 hours in a CO_2 incubator. Following incubation, the culture medium was replaced with the sample solution as described above. The cells were then treated for an additional 24 hours. Cell viability was assessed using the MTT assay. A volume of 10 µL of 3-(4,5-dimethylthiazol-2-yl)-2,5-diphenyltetrazolium bromide (MTT) was added to each well, followed by 3 hours of incubation at 37°C in 5% CO_2. Subsequently, 100 µL of dimethyl sulfoxide (DMSO) was added to each well to solubilize the formazan crystals. Absorbance was measured at 570 nm using a microplate reader (InfiniteRM200 NanoQuant, TECAN, Switzerland). All assays were performed in triplicate, and cell viability was calculated using the following equation 2.

$$\text{Cell viability (\%)} = \frac{(\text{sample}-\text{blank})}{(\text{control}-\text{blank})} \times 100\% \qquad (2)$$

2.2.4.4 Cytoprotective assay

For cytoprotective evaluation, HaCaT cells were exposed to UVB irradiation for 6 hours at a distance of 15 cm. An external control group was not exposed to UVB radiation. Cell viability was then assessed using the MTT assay as previously described in section 2.2.4.3.

3. Results and Discussion

The XRD analysis results indicate that the AuNPs are pure, Fig. 1. This is evidenced by the diffraction patterns observed at 2θ angles of 38.20°, 44.37°, 64.49°, 77.62°, and 81.75°, corresponding to the (111), (002), (022), (113), and (222) planes, respectively, which match the cubic crystal structure of Au (reference data COD No. 1100138). A noticeable difference in the peak intensity of the (111) plane was observed, suggesting a variation in crystal size. Therefore, the full width at half maximum (FWHM) was calculated to examine the crystal structure. The crystallite size was determined using the Debye-Scherrer method (Equation 3, and the calculated crystallite sizes are presented in Table 1.

$$D = \frac{0.9\lambda}{\beta \cos\theta} \qquad (3)$$

Where D is the crystallite size, λ is the wavelength of CuKα1 radiation, β is the FWHM of the (111) diffraction peak, and θ is the Bragg angle.

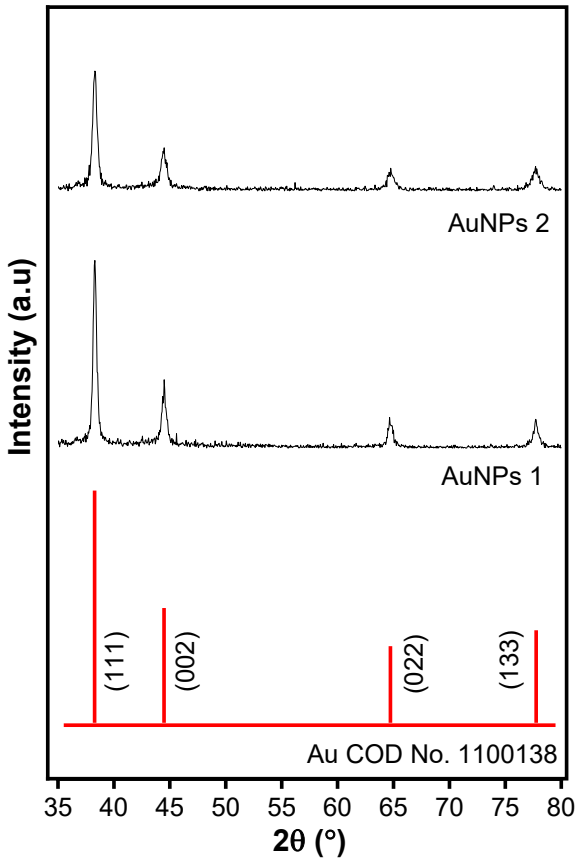

Figure 1. XRD patterns of AuNPs synthesized in different supporting electrolyte solutions.

The crystallite size of AuNPs 1 was slightly smaller, likely due to the presence of sulfate ions (SO_4^{2-}), which hindered the transport of gold ions (Au^{3+}) and gold atoms (Au) to the electrode, thereby suppressing nucleation growth and leading to a reduction in crystallite size [26].

Table 1. Crystallite size of AuNPs.

Sample	FWHM (111)	Crystallite size (nm)
AuNPs 1	0.338	25.5
AuNPs 2	0.417	20.0

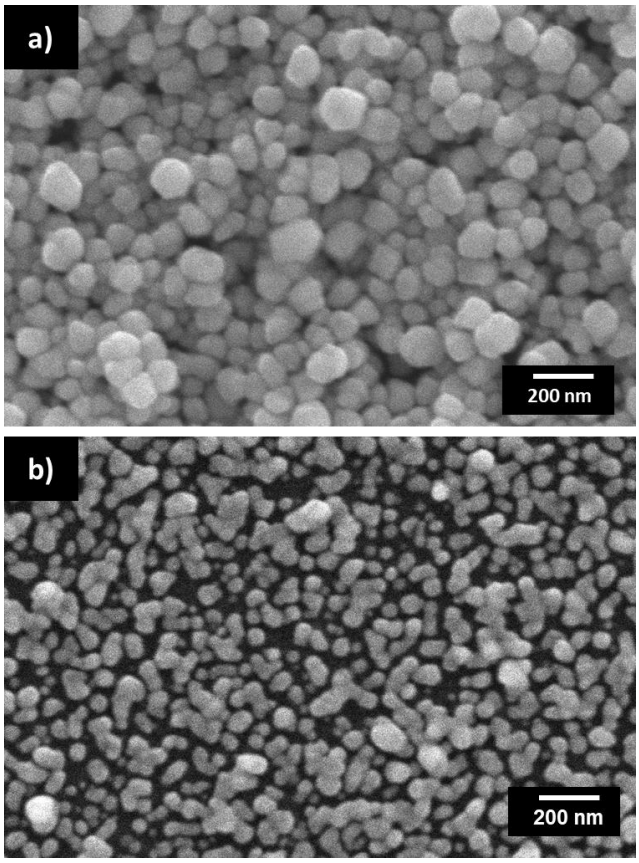

Figure 2. Top surface SEM micrograph of AuNPs synthesized in (a) KCl and (b) Na_2SO_4 electrolytes.

Figure 2 shows the morphology of AuNPs synthesized in different supporting electrolyte solutions. AuNPs 1 exhibit a spherical morphology, whereas AuNPs 2 display a rounded morphology. Furthermore, AuNPs 1 possess a higher particle density compared to AuNPs 2. This disparity in particle density arises from the influence of the electrolyte ions. During the AuNPs deposition process, two different anions play a role in the dynamics of particle nucleation and growth, specifically Cl^- ions in AuNPs 1 and SO_4^{2-} ions in AuNPs 2 [27]. The Cl^- ions generate a weaker electrostatic repulsion between ions, thereby facilitating a more rapid particle core growth process as these ions do not sufficiently impede Au ion transport. Meanwhile, SO_4^{2-} ions exert a stronger electrostatic repulsion, which hinders Au ions transport [28]. Moreover, the elevated concentration of Cl^- ions in the solution, originating from both the precursor and the electrolyte, is capable of yielding a high electrolyte conductivity, consequently enhancing the current, providing nucleation acceleration, and resulting in more uniform particles.

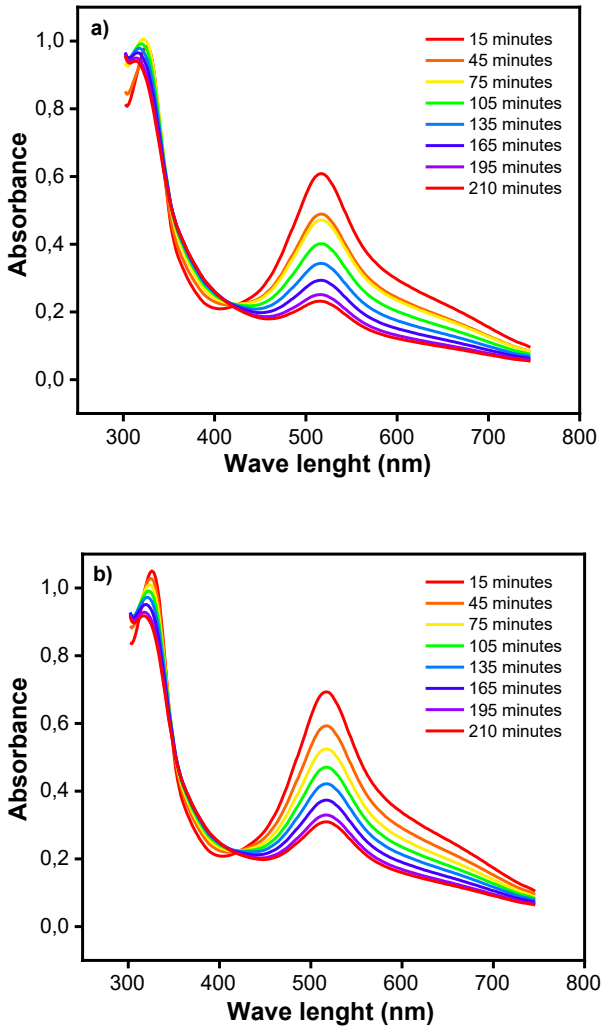

Figure 3. Absorbance spectrum of DPPH form antioxidant test (a) AuNPs 1 and (b) AuNPs 2.

The antioxidant activity of AuNPs against DPPH free radicals was assessed by analyzing the absorbance spectrum of DPPH solution after incubation with AuNPs. As shown in Fig. 3, the DPPH absorbance peak was detected at 516 nm [29]. The absorbance value was decreased proportionally with incubation duration, indicating that AuNPs perform as antioxidants, neutralizing DPPH molecules [30]. During incubation, an electron was transferred from the free electron on the nitrogen atom

(N) of DPPH to the electropositive Au atom [31]. The formation of an Au-DPPH complex via a coordinate covalent bond caused a shift in the absorption wavelength and a decrease in intensity at 516 nm [29].

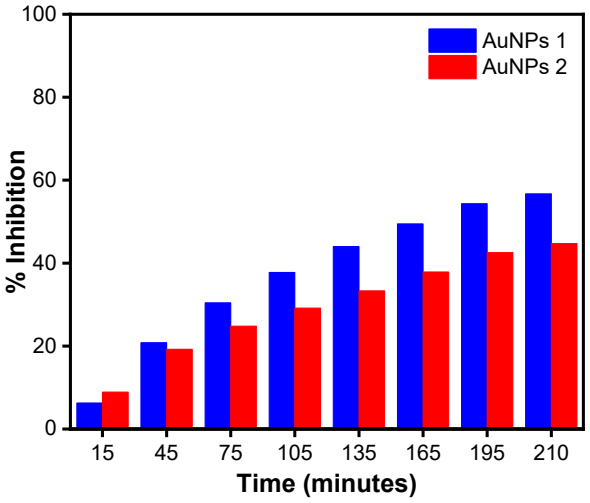

Figure 4. Percent inhibition of AuNPs DPPH test.

.The efficacy of AuNPs in scavenging DPPH free radicals is represented by the percentage inhibition. Figure 4 demonstrates that AuNPs 1 exhibit a comparatively superior antioxidant performance to AuNPs 2. The elevated particle density of AuNPs 1 correlates with enhanced antioxidant activity. This high particle density provides a larger surface area with a higher number of active sites, thereby augmenting the adsorption of DPPH molecules within a given area [32]. These results are related to our previous research, which is that the DPPH absorption of AuNPs depends on the number of particles [33].

Further investigations were conducted to assess the biocompatibility of AuNPs 1. The test must be provided due to its potential cytotoxicity of AuNPs associated with their small particle size and higher reactivity compared to larger-sized particles [34,35]. To evaluate the biocompatibility of AuNPs 1, cytotoxicity and cytoprotective assays were performed. Prior to the cytoprotective assay, a cytotoxicity test was conducted to determine the concentration of gold nanoparticles that is safe for cellular applications.

The results of the cytotoxicity and cytoprotective assay are presented in Fig. 5. The results indicate that the gold nanoparticles exhibit better cytocompatibility compared to the negative control, fluorouracil (FU), with a cell viability rate of 67.16%. This suggests that AuNPs 1 are non-toxic and safe for cells. Moreover, the cytoprotective assay demonstrated that AuNPs 1 can protect cells from free radicals generated by UV irradiation. As shown in Figure 5b, the cytoprotective activity of AuNPs 1 reached 102.66%, which is slightly higher than that of vitamin C. These findings suggest that AuNPs 1 may serve as a promising candidate for antioxidant applications.

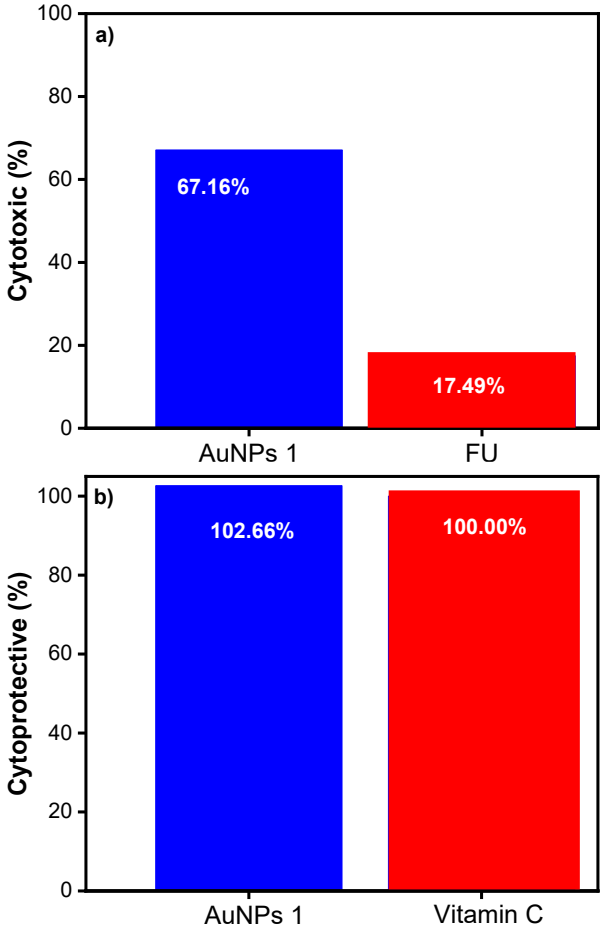

Figure 5. (a) Cytotoxicity of AuNPs 1 compared with FU (control) and (b) cytoprotective of AuNPs 1 compared with vitamin C (control).

4. Conclusion

The electrolytes KCl and Na_2SO_4 significantly influenced the growth dynamics of AuNPs. The electrostatic forces exerted by chloride (Cl^-) and sulfate (SO_4^{2-}) anions played a critical role in determining particle density. The larger sulfate anions, with stronger electrostatic repulsion, effectively suppressed particle growth. In contrast, the smaller chloride anions, exhibiting weaker electrostatic interactions, minimally inhibited growth and enhanced electrolyte conductivity, thereby promoting faster nucleation and improved particle uniformity. The higher particle density of AuNPs 1 correlated with its enhanced DPPH inhibition (56.70%) compared to AuNPs 2 (44.70%). The cytotoxic and cytoprotective activities of AuNPs 1 were 67.16% and 102.66%, respectively, demonstrating that the

AuNPs are biocompatible and have antioxidant activity for cells.

Author Contributions

B. Asih Suliasih: Conceptualization, funding acquisition, methodology, supervision, visualization, writing – original draft, Charzen Mae Kinoan: Investigation, writing – review & editing.

Conflict of Interest

There is no conflict of interest to declare.

Acknowledgement

The authors acknowledge support from the National University of Malaysia facilitated sample characterizations.

References

[1] N. Chandimali, S.G. Bak, E.H. Park, H.J. Lim, Y.S. Won, E.K. Kim, S.I. Park, S.J. Lee, Free radicals and their impact on health and antioxidant defenses: a review, *Cell Death Discov*. **11** (2025). https://doi.org/10.1038/s41420-024-02278-8.

[2] S.G. Tumilaar, A. Hardianto, H. Dohi, D. Kurnia, A Comprehensive Review of Free Radicals, Oxidative Stress, and Antioxidants: Overview, Clinical Applications, Global Perspectives, Future Directions, and Mechanisms of Antioxidant Activity of Flavonoid Compounds, *J Chem*. **2024** (2023). https://doi.org/10.1155/2024/5594386.

[3] K. Lu, S. Guo, Z. Tan, H. Wang, D. Shang, Y. Liu, X. Li, Z. Wu, M. Hu, Y. Zhang, Exploring atmospheric free-radical chemistry in China: The self-cleansing capacity and the formation of secondary air pollution, *Natl Sci Rev*. **6** (2019) 579–594. https://doi.org/10.1093/nsr/nwy073.

[4] A. Elsayed Azab, Almokhtar A Adwas, A.S. Ibrahim Elsayed, A. A Adwas, Ata Sedik Ibrahim Elsayed, F.A. Quwaydir, Oxidative stress and antioxidant mechanisms in human body, *Journal of Applied Biotechnology & Bioengineering*. **6** (2019) 43–47. https://doi.org/10.15406/jabb.2019.06.00173.

[5] G. Martemucci, C. Costagliola, M. Mariano, L. D'andrea, P. Napolitano, A.G. D'Alessandro, Free Radical Properties, Source and Targets, Antioxidant Consumption and Health, *Oxygen*. **2** (2022) 48–78. https://doi.org/10.3390/oxygen2020006.

[6] T. Yoshikawa, F. You, Oxidative Stress and Bio-Regulation, *Int J Mol Sci*. **25** (2024). https://doi.org/10.3390/ijms25063360.

[7] K. Jomova, S.Y. Alomar, S.H. Alwasel, E. Nepovimova, K. Kuca, M. Valko, Several lines of antioxidant defense against oxidative stress: antioxidant enzymes, nanomaterials with multiple enzyme-mimicking activities, and low-molecular-weight antioxidants, *Arch Toxicol*. **98** (2024) 1323–1367. https://doi.org/10.1007/s00204-024-03696-4.

[8] K. Lalhminghlui, G.C. Jagetia, Evaluation of the free-radical scavenging and antioxidant activities of Chilauni, Schima wallichii Korth in vitro, *Future Sci OA*. **4** (2018). https://doi.org/10.4155/fsoa-2017-0086.

[9] J. Flieger, W. Flieger, J. Baj, Antioxidants : Classification , Natural Sources , Activity / Capacity, *Materials*. **14** (2021) 1–54. https://www.mdpi.com/journal/materials.

[10] R. Amarowicz, R.B. Pegg, Natural antioxidants of plant origin, 1st ed., Elsevier Inc., 2019. https://doi.org/10.1016/bs.afnr.2019.02.011.

[11] T.A. Uzombah, T.A. Uzombah, The Implications of Replacing Synthetic Antioxidants with Natural Ones in the Food Systems, *Natural Food Additives*. (2022). https://doi.org/10.5772/INTECHOPEN.103810.

[12] C.S. Yang, C.T. Ho, J. Zhang, X. Wan, K. Zhang, J. Lim, Antioxidants: Differing Meanings in Food Science and Health Science, *J Agric Food Chem*. **66** (2018) 3063–3068. https://doi.org/10.1021/ACS.JAFC.7B05830/ASSET/IMAGES/MEDIUM/JF-2017-05830M_0004.GIF.

[13] X. Xu, A. Liu, S. Hu, I. Ares, M.R. Martínez-Larrañaga, X. Wang, M. Martínez, A. Anadón, M.A. Martínez, Synthetic phenolic antioxidants: Metabolism, hazards and mechanism of action, *Food Chem*. **353** (2021) 129488. https://doi.org/10.1016/J.FOODCHEM.2021.129488.

[14] W. Najahi-Missaoui, R.D. Arnold, B.S. Cummings, Safe Nanoparticles: Are We There Yet?, *Int J Mol Sci*. **22** (2020) 1–22. https://doi.org/10.3390/IJMS22010385.

[15] M. Mitra, Applications and Properties of Gold Nanoparticles, *Nano Particle*. **1** (2019). https://doi.org/10.35702/NANO.10004.

[16] B.A. Suliasih, S. Budi, H. Katas, Synthesis and application of gold nanoparticles as antioxidants, *Pharmacia*. **71** (2024) 1–19. https://doi.org/10.3897/PHARMACIA.71.E112322.

[17] A. Karnwal, R.S. Kumar Sachan, I. Devgon, J. Devgon, G. Pant, M. Panchpuri, A. Ahmad, M.B. Alshammari, K. Hossain, G. Kumar, Gold Nanoparticles in Nanobiotechnology: From Synthesis to Biosensing Applications, *ACS Omega*. **9** (2024) 29966–29982. https://doi.org/10.1021/acsomega.3c10352.

[18] B.A. Suliasih, A. Sakinah, Marissa Angelina, The Effect of Electrodeposition Voltage on the Antioxidant Activity of Gold Nanoparticles,

Chemistry and Materials. **3** (2024) 27–33. https://doi.org/10.56425/cma.v3i1.72.

[19] C.J. Weber, N.E. Strom, O. Simoska, Electrochemical deposition of gold nanoparticles on carbon ultramicroelectrode arrays, *Nanoscale*. **16** (2024) 16204–16217. https://doi.org/10.1039/d4nr02326a.

[20] S.A. Lee, J.W. Yang, S. Choi, H.W. Jang, Nanoscale electrodeposition: Dimension control and 3D conformality, *Exploration*. **1** (2021). https://doi.org/10.1002/EXP.20210012.

[21] S. Budi, B.A. Suliasih, I.D. Fikri, Afrizal, M. Angelina, Developing antioxidant of gold nanofilm by a facile electrodeposition method, *J Adv Pharm Technol Res*. **15** (2024) 320–325. https://doi.org/10.4103/JAPTR.JAPTR_138_24.

[22] N.D. Zakaria, M.H. Omar, N.N. Ahmad Kamal, K. Abdul Razak, T. Sönmez, V. Balakrishnan, H.H. Hamzah, Effect of Supporting Background Electrolytes on the Nanostructure Morphologies and Electrochemical Behaviors of Electrodeposited Gold Nanoparticles on Glassy Carbon Electrode Surfaces, *ACS Omega*. **6** (2021) 24419–24431. https://doi.org/10.1021/acsomega.1c02670.

[23] W. Zhang, X. Chen, Y. Wang, L. Wu, Y. Hu, Experimental and Modeling of Conductivity for Electrolyte Solution Systems, *ACS Omega*. **5** (2020) 22465–22474. https://doi.org/10.1021/acsomega.0c03013.

[24] G. Yang, G. Ma, M. He, X. Ji, W. Li, H.J. Youn, H.L. Lee, J. Chen, Comparison of Effects of Sodium Chloride and Potassium Chloride on Spray Drying and Redispersion of Cellulose Nanofibrils Suspension, *Nanomaterials*. **11** (2021) 439. https://doi.org/10.3390/nano11020439.

[25] L. Van Sang, T.T.T. Huong, L.N.T. Minh, Molecular dynamics simulations of the melting of KCl nanoparticles, *The European Physical Journal D*. **68** (2014) 292. https://doi.org/10.1140/epjd/e2014-40454-7.

[26] K. Nieszporek, J. Nieszporek, Molecular dynamics simulation of an aqueous Na2SO4 solution, *Annales Universitatis Mariae Curie-Sklodowska, Sectio AA – Chemia*. **72** (2018) 67–76. https://doi.org/10.17951/AA.2017.72.2.67-76.

[27] S. Li, X. Dong, Y. Zhao, J. Mao, W. Chen, A. Chen, Y. Song, G. Li, Z. Jiang, W. Wei, Y. Sun, Chloride Ion Adsorption Enables Ampere-Level CO_2 Electroreduction over Silver Hollow Fiber, *Angewandte Chemie*. **134** (2022) e202210432. https://doi.org/10.1002/ANGE.202210432.

[28] M. Kulichenko, N. Fedik, K. V. Bozhenko, A.I. Boldyrev, Hydrated Sulfate Clusters SO 42- (H 2 O) n (n = 1-40): Charge Distribution Through Solvation Shells and Stabilization, *Journal of Physical Chemistry B*. **123** (2019) 4065–4069. https://doi.org/10.1021/ACS.JPCB.9B01744/SUPPL_FILE/JP9B01744_SI_001.PDF.

[29] S. Kandi, A.L. Charles, Statistical comparative study between the conventional DPPH [rad] spectrophotometric and dropping DPPH [rad] analytical method without spectrophotometer: Evaluation for the advancement of antioxidant activity analysis, *Food Chem*. **287** (2019) 338–345. https://doi.org/10.1016/J.FOODCHEM.2019.02.110.

[30] F. Avelino, 2,2-Diphenyl-1-picrylhydrazyl (DPPH)., in: Antioxidant Methods, Elsevier, 2024: pp. 79–93. https://doi.org/10.1016/B978-0-443-21591-9.00006-8.

[31] T. Endo, T. Fukunaga, T. Yoshimura, K. Esumi, Scavenging DPPH radicals catalyzed by binary noble metal-dendrimer nanocomposites, *J Colloid Interface Sci*. **302** (2006) 516–521. https://doi.org/10.1016/J.JCIS.2006.06.053.

[32] Y. Ma, G. Nagy, M. Siebenbürger, R. Kaur, K.M. Dooley, B. Bharti, Adsorption and Catalytic Activity of Gold Nanoparticles in Mesoporous Silica: Effect of Pore Size and Dispersion Salinity, *Journal of Physical Chemistry C*. **126** (2022) 2531–2541. https://doi.org/10.1021/acs.jpcc.1c09573.

[33] B.A. Suliasih, A. Sakinah, Marissa Angelina, The Effect of Electrodeposition Voltage on the Antioxidant Activity of Gold Nanoparticles, *Chemistry and Materials*. **3** (2024) 27–33. https://doi.org/10.56425/cma.v3i1.72.

[34] A. Sani, C. Cao, D. Cui, Toxicity of gold nanoparticles (AuNPs): A review, *Biochem Biophys Rep*. **26** (2021). https://doi.org/10.1016/j.bbrep.2021.100991.

[35] M. Kus-liśkiewicz, P. Fickers, I. Ben Tahar, Biocompatibility and cytotoxicity of gold nanoparticles: Recent advances in methodologies and regulations, *Int J Mol Sci*. **22** (2021). https://doi.org/10.3390/ijms222010952.